Decoration lattices of colloids adsorbed on stripe-patterned substrates

H. M. Harreis,* M. Schmidt, and H. Löwen
Institut für Theoretische Physik II, Heinrich-Heine-Universität Düsseldorf, Universitätsstraße 1, D-40225 Düsseldorf, Germany
(Received 27 November 2001; published 26 March 2002)

The equilibrium structure of decoration lattices composed of colloidal particles adsorbed on periodic stripe-patterned substrates is calculated as a function of the stripe width and separation and for different interparticle interactions. Due to a competition of length scales, a wealth of different stable decoration lattices occurs such as triangular, quadratic, rhombic, kitelike, and sheared honeycomb lattices, triangular slices as well as triangle superlattices. This is of relevance for constructing templates that enforce crystal growth of unusual solid structures.

DOI: 10.1103/PhysRevE.65.041602 PACS number(s): 67.70.+n, 82.70.Dd, 68.43.−h, 68.08.Bc

I. INTRODUCTION

Recent advances in microfabrication have allowed to prepare chemically or topographically patterned substrates in a controlled way by using e.g., lithographic printing or other etching techniques [1,2]. There is a profound influence of such a substrate pattern on wetting [3–10], on adsorption of soft matter [11,12] and biological macromolecules [13,14], on crystal nucleation [15], and on bulk phase transitions such as freezing [16,17] and fluid-fluid phase separation [18]. Patterned substrates have also been used in so-called microfluidics in order to control chemical reactions on a microscale or nanoscale [19,20]. For this purpose, one-dimensional channels are considered that carry the reacting material. These channels can either be attractive stripes or topographical groves.

In this paper we study the adsorption of colloidal particles on a sticky periodic stripelike pattern. Our motivation to do so is first coming from experiments where decorations were obtained by adsorbing colloidal spheres on a patterned substrate mask [11,21–29], or in an external laser field [30], for a recent review see Ref. [31]. Such a decorated substrate may be offered as a template to other mobile colloidal particles in order to nucleate further colloidal crystalline sheets and to grow ''exotic'' colloidal bulk crystals [16,32,33]. The colloidal particles can both be sterically stabilized [34] or charge stabilized. In the former case, the pattern can be prepared by a different chemical coating while in the latter the surface pattern is dictated by the inhomogeneous surface charge density [13,35,36]. Another experimental system to observe structure formation near interfaces is magnetic bubble arrays with periodic line pinning [37]. While much experience has been accumulated in how to prepare the substrate in order to realize a prescribed mask, a more systematic theoretical understanding of possible decoration structures as induced by an underlying sticky periodic pattern is missing. In this paper we investigate this problem for a periodic stripe pattern within a simple model calculation including both attractive and repulsive effective interparticle interactions. In equilibrium, we discover a wealth of possible stable decoration lattices. Hence although the substrate pattern is relatively simple, the decoration can be fascinatingly complex so that a wide range of decoration structures can be generated in a controlled and simple way. Even for a single stripe, periodic decoration structures as buckled alternating superlattices with a unit cell involving a large triangle of particles and finite slices of a triangular bulk lattice may become stable. For a periodic stripe pattern, there are even more stable decoration lattices, involving triangular, quadratic, rhombic, kitelike, and sheared honeycomb lattices.

The paper is organized as follows: We describe the model in Sec. II and outline our theory in Sec. III. Results are presented in Sec. IV, and we conclude in Sec. V.

II. THE MODEL

We consider a periodically stripe-patterned smooth surface, shown schematically in Fig. 1. The width of the sticky stripes is d, while the distance between neighboring stripes is b, so that the structure is periodic in a direction perpendicular to the stripes with periodicity length $b+d$. This patterned surface is exposed to a suspension of spherical colloidal particles with hard-core diameter σ aggregating onto the pattern. An aggregated sphere exhibits a point contact with the substrate gaining a potential energy $-\epsilon<0$, provided the contact point is inside a sticky stripe. We assume strongly attractive substrates, such that ϵ is much larger than the ther-

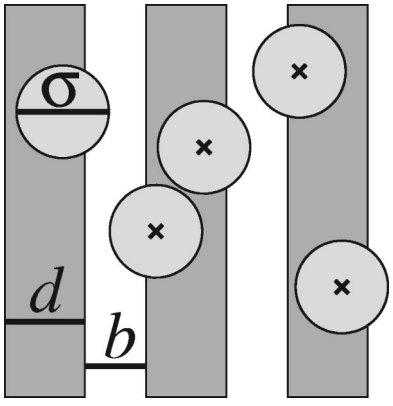

FIG. 1. Model of hard spheres of diameter σ on an attractive stripe pattern (dark gray) of width d and interstripe distance b. The sphere centers (crosses) are constrained to lie inside the stripes.

*Email address: harreis@thphy.uni-duesseldorf.de

mal energy k_BT. Aggregation on the interstripe regions is neglected. Aggregation occurs from a dilute bulk solution of colloids. Here, we do not discuss the dynamics of aggregation or deposition [38], but rather focus on the equilibrium structure present after relaxation of the adsorption process. Typical pair potentials $V(r)$ as a function of separation distance r between colloids have an inner hard core and a short-ranged tail. By addition of nonadsorbing polymers or salt ions to the bulk solution, both attractive or repulsive tails can be realized [39]. For simplicity, we use a square-well/square-shoulder potential,

$$V(r)=\begin{cases}\infty & \text{for} \quad r<\sigma,\\ v_0 & \text{for} \quad \sigma\leqslant r<\sigma(1+\delta),\\ 0 & \text{else,}\end{cases} \tag{1}$$

with a small positive (reduced) range δ. Depending on the sign of v_0, the tail is either repulsive ($v_0>0$) or attractive ($v_0<0$). Thermodynamics of this system in bulk has been studied in detail, see e.g., Refs. [40–43] and references therein. Here, we expose the model to an inhomogeneous surface, and restrict ourselves to zero temperature, i.e., to the classical ground state [44]. Let A be the area of the surface, N be the number of adsorbed particles, $\rho=N/A$ denote the (two-dimensional) number density, and $\eta=\pi\rho\sigma^2/4$ the corresponding area fraction. The whole system is characterized by four reduced parameters, namely, the reduced width d/σ of the attractive stripe, the reduced interstripe width b/σ, the range of the potential δ, and the ratio v_0/ϵ of colloid-colloid to substrate-colloid interaction.

III. THEORY

For zero temperature the energetically most favorable configurations of the adsorbate will be attained. Technically, we need to minimize the total potential energy U per substrate area A. One may decompose $u\equiv U/A=u_1+u_2$, where u_1 stems from substrate-particle attraction, and u_2 from particle-particle interactions. These contributions are

$$u_1=-\epsilon\rho, \tag{2}$$

$$u_2=A^{-1}\sum_{i=1}^{N}\sum_{j=i+1}^{N} V(|\vec{r}^{(i)}-\vec{r}^{(j)}|), \tag{3}$$

where $\vec{r}^{(i)}$ denote (two-dimensional) particle positions on the surface. It will prove useful to rewrite u_2 in terms of the *kissing numbers* $k^{(i)}$ (of particle i), that equal the number of touching spheres (i.e., $|\vec{r}^{(i)}-\vec{r}^{(j)}|=\sigma$) for particle i. If we assume absence of hard-core overlap, and all particle separations r being either at contact ($r=\sigma$), or outside the range of interaction [$r>\sigma(1+\delta)$], we can write

$$u_2=\frac{v_0}{2A}\sum_{i=1}^{N} k^{(i)}\equiv v_0\rho k/2, \tag{4}$$

where $k=N^{-1}\Sigma_{i=1}^{N}k^{(i)}$ is the (over system) averaged kissing number. Note that u_1 favors optimal packing of spheres, while u_2 couples to the number of sphere contacts. Decisive for phase behavior is the competition between optimization of packing and kissing, where the ratio v_0/ϵ is a control parameter. In practice, we start with different candidate lattices for the colloids, calculate u for each one in order to find the optimal lattice that minimizes u. The choice of candidates is motivated by mathematical packing and includes rhombic, square, triangular, kite, and other structures involving superlattices. We disregard the disordered fluid phase, as temperature is zero. We have not considered nonperiodic structures as quasicrystals [45], that are expected to be unfavorable for a one-component colloidal system, but could become relevant for binary and ternary mixtures. A similar zero-temperature calculation on structured substrates can be found in Ref. [44], for quadratic substrate patterns and Lennard-Jones interparticle interactions. We further remark that similar crystalline lattice structures were obtained in Ref. [46] for a different physical system, namely, flux lattices in layered superconductors. In contrast to the short-range interactions employed in the present paper, the interaction between flux lines is long ranged.

IV. RESULTS

A. Single stripe

For $b/\sigma>1+\delta$, the spheres adsorbed on neighboring stripes are decoupled and the problem reduces to that of adsorption onto a single stripe. For simplicity, we let $\delta\to 0$ and $v_0\leqslant 0$, so that we deal with sticky hard spheres. Geometrical considerations as well as numerically checking other structures makes it possible for us to restrict the actually realized candidates to two n-layered crystals, namely (i) triangular lattices ($n\Delta$), and (ii) *supertriangle* structures ($n\mathcal{S}$), see Fig. 2 for illustrations. $n\Delta$ is a portion of the triangular (bulk) lattice. The $n\mathcal{S}$ crystal consists of a buckled superlattice of alternating close-packed triangles.

The relevant properties of both candidates are the following. For n close-packed layers on a stripe of width d, we find

$$\rho_\Delta=\frac{n}{d\sigma}, \tag{5}$$

$$\rho_{\mathcal{S}}=\frac{n(n+1)}{d\sigma[(n-1)+2\cos\alpha]}, \tag{6}$$

where $\alpha\in[0,\pi/3)$ is the mismatch angle between adjacent supertriangles, see Fig. 2. For close-packed states, α is related to d via

$$\alpha(d)=\arcsin[d-\sqrt{3}(n-1)/2]. \tag{7}$$

Note that for $\alpha=0$ (no mismatch), $n\Delta$ coincides with $n\mathcal{S}$, and trivially $\rho_\Delta=\rho_{\mathcal{S}}$. These configurations define the close-packed area fraction η_{cp} plotted in Fig. 3(a) as a function of stripe width d. For the average kissing number, we obtain via counting of sphere contacts,

$$k_\Delta=6-\frac{4}{n}, \tag{8}$$

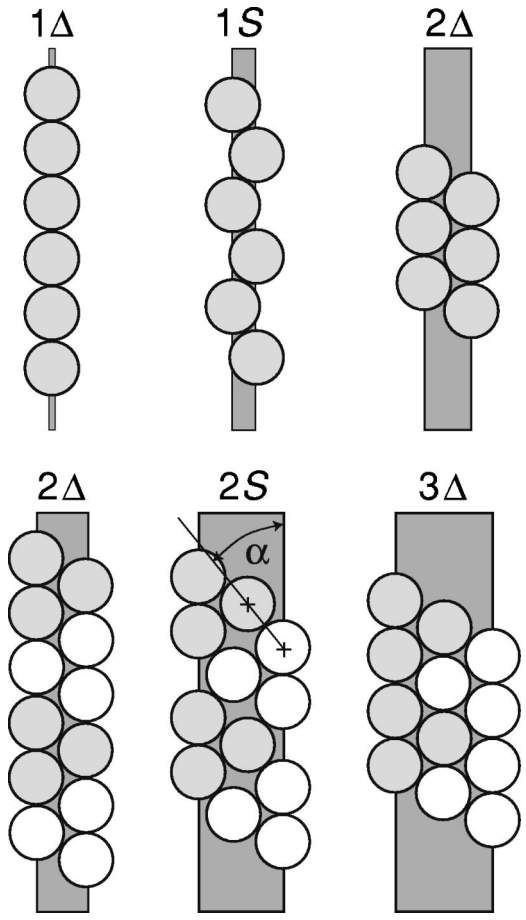

FIG. 2. Crystal structures $n\Delta$ and $n\mathcal{S}$ of hard spheres sticking to a single stripe of width d for $n=1,2,3$. The stripe width d increases from left to right. $\alpha\in[0,\pi/3)$ is the mismatch angle between adjacent supertriangles. Spheres building equilateral (super)triangles are shaded to guide the eye. For larger d the sequence continues in an analogous way.

$$k_{\mathcal{S}}=6-\frac{8}{n+1}. \tag{9}$$

Although in the limit $\alpha\to 0$ the structures themselves become identical, $k_{\mathcal{S}}$ does not approach k_{Δ} smoothly, but jumps at $\alpha=0$. Relevant for the potential energy [Eq. (4)] is not the kissing number alone, but $\rho k/2$, that is plotted in Fig. 3(b) as a function of stripe width d.

In the limit $v_0\to-\infty$, maximal kissing *per unit area* determines the equilibrium structure, as the dominant contribution $\rho k/2$ [Eq. (4)] to the energy u is to be maximized. Quite surprisingly, in each interval $n\sqrt{3}\sigma/2<d<(n+1)\sqrt{3}\sigma/2$, a transition $n\Delta\to n\mathcal{S}$ exists, that is located at $d/\sigma=(n-1)\sqrt{3}/2+\sqrt{1-[(2-n^{-1})/(3-2n^{-1})]^2}$, where large k and low ρ in $n\Delta$ are outperformed by low k and high ρ in $n\mathcal{S}$. Note that as $n\to\infty$, the transition persists, and the relative phase transition point $d/\sigma-(n-1)\sqrt{3}/2$ approaches $\sqrt{5}/3=0.7454$.

Putting things together, we can turn to the full energetically driven phase diagram for arbitrary $|v_0/\epsilon|$. Asking first how additional layers $n\to n+1$ jump in, we find the simple

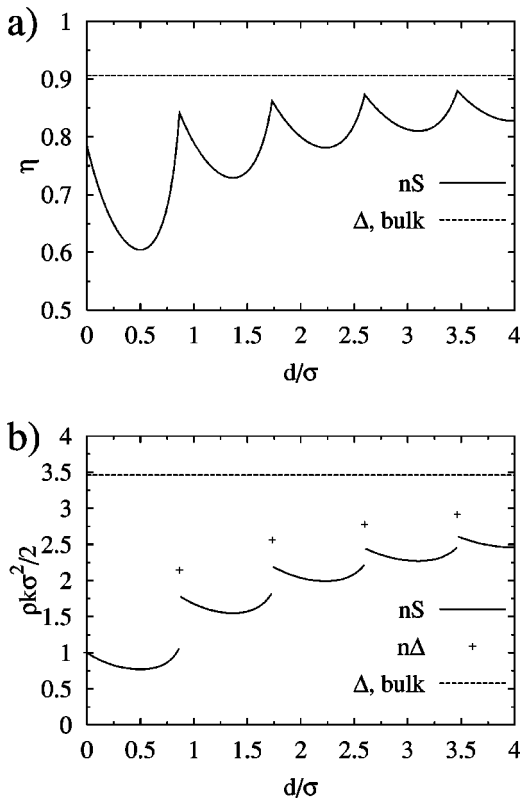

FIG. 3. Relevant densities for close-packed hard spheres of diameter σ on a stripe of width d as a function of d/σ for $n\Delta$ (symbols) and $n\mathcal{S}$ (lines) structures, as well as for the bulk triangular lattice (dashed lines). (a) Area packing fraction η. (b) Kissing number density per unit area, $\rho\sigma^2k/2$.

answer: A transition $n\mathcal{S}\to(n+1)\Delta$ is located at $d=n(\sqrt{3}/2)\sigma$, *independent* of v_0/ϵ. The $n\Delta\to n\mathcal{S}$ transition is less trivial. We obtain

$$d=(n-1)(\sqrt{3}/2)\sigma+\sigma\sqrt{1-\left[\frac{(\epsilon/v_0)-2+n^{-1}}{(\epsilon/v_0)-3+2n^{-1}}\right]^2}. \tag{10}$$

In the limiting cases, for $v_0/\epsilon=0$, we recover the close-packing structure of discs between lines, and for $v_0/\epsilon\to-\infty$ the structure with maximal number of kisses. Equation (10) interpolates smoothly between these limits.

The resulting phase diagram is shown in Fig. 4 as a function of d and $\exp(v_0/\epsilon)$. We restrict ourselves to $n\leqslant 4$; the succession of $n\mathcal{S}$ and $n\Delta$ continues for larger d. In the limit of broad stripes ($d\to\infty$) and infinitely many layers ($n\to\infty$), we consider $d-(n-1)(\sqrt{3}/2)\sigma$, that maps d/σ onto the $[0,1]$ interval and obtain the universal (n-independent) result,

$$d-(n-1)(\sqrt{3}/2)\sigma\to\sigma\sqrt{\frac{5-2(\epsilon/v_0)}{[(\epsilon/v_0)-3]^2}}. \tag{11}$$

Narrow stripes with $0<d<(\sqrt{3}/2)\sigma$ constitute a special case, because of dominance of a single phase $1\mathcal{S}$ (1Δ is

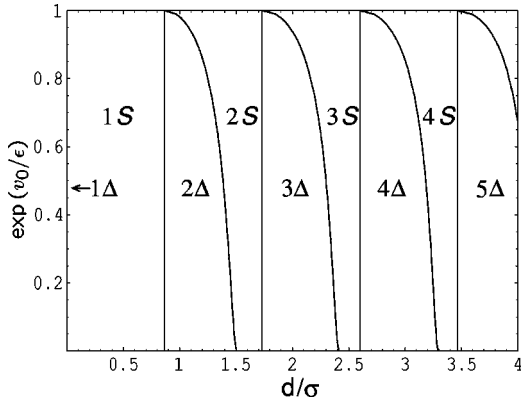

FIG. 4. Phase diagram for sticky hard spheres adsorbed on a single sticky stripe as a function of reduced stripe width d/σ, and the (exponentiated) ratio v_0/ϵ of interparticle versus substrate potential. Lines are phase boundaries between $n\Delta$ and $n\mathcal{S}$ structures. The 1Δ phase is a vertical line at $d/\sigma=0$.

squeezed to a vertical line at $d=0$.) The reason for this behavior is that 1Δ and $1\mathcal{S}$ possess equal kissing numbers. This is in contrast to $n>1$, where $k_\Delta > k_\mathcal{S}$.

Two remarks are in order: First, the supertriangular phases $n\mathcal{S}$ are the two-dimensional analog of three-dimensional prism phases [47] found for hard spheres confined between parallel hard plates. A similar cascade of phases has been found there, although this is interrupted by other additional phases such as a rhombic structure [48,49]. Second, in contrast to the bulk problem [50,51], we are not aware of a strict mathematical proof for close-packed configurations, nor of any other numerical investigation of the packing problem of discs between lines. Other confining geometries such as the square [52–54], triangles [55,56], and the circle [57–59] have been treated in a rigorous way.

B. Coupled stripes

For $b/\sigma < 1+\delta$, particles on adjacent stripes interact. We limit ourselves to the hard sphere case, $\delta=0$, and hence deal with a packing problem. To break possible degeneracy of close-packed states, we consider $v_0/\epsilon \to 0^-$, favoring sphere contacts.

1. Triangular lattice

We focus on the close-packed triangular lattice, of which is known that there is no denser structure in bulk. If we succeed to identify patterns that are compatible (all lattice sites lie on sticky stripes) with the triangular lattice, we have then *proved* that there is no denser decoration lattice. The task is to determine the (b,d) regimes in which the triangular lattice is geometrically possible. Let the lattice sites of a triangular lattice be

$$\vec{A}(j,k) = j\vec{a}_1 + k\vec{a}_2, \quad j,k = 0,\pm 1,\pm 2,\ldots, \tag{12}$$

where $\vec{a}_1=(\sigma,0), \vec{a}_2=(\sigma/2,\sqrt{3}\sigma/2)$ are basis vectors. In the following, we imagine the lattice to be fixed on the surface and attempt to determine those stripe patterns that are compatible with the particle lattice. For given b,d the pattern is determined by the orientation along the stripes. This orientation may be expressed as $\vec{A}(j,k)/|\vec{A}(j,k)|$, with suitably chosen values for j,k. In order to find stripe patterns that fit the lattice, we calculate the distance $\xi(j,k)$ between adjacent lattice lines (the analog to lattice *planes* in three dimensions), that are parallel to $\vec{A}(j,k)/|\vec{A}(j,k)|$. To this end, we introduce a vector $\vec{B}(j,k)$, that is orthogonal to $\vec{A}(j,k)/|\vec{A}(j,k)|$ as

$$\vec{B}(j,k) = -(j+2k)\vec{a}_1 + (2j+k)\vec{a}_2. \tag{13}$$

Projection of $(-1/k)\vec{a}_1$ onto $\vec{B}$ gives the lattice line distance

$$\xi(j,k) = -\frac{\vec{a}_1\cdot\vec{B}}{k|\vec{B}|} = \frac{\sqrt{3}\sigma/2}{\sqrt{j^2+jk+k^2}}. \tag{14}$$

Upon varying j and k, the argument j^2+jk+k^2 generates a (seemingly irregular when sorted) sequence of integer numbers, namely, 1,3,4,7,9,12,13,16,19,21,25,27,28,31,36,37, 39,43,48,49, ... Expression (14) gives the lattice line distance for an orientation of lattice lines (parallel to the stripes) defined by j,k. Assuming that $b+d$ and the lattice structure $\xi(j,k)$ have the same periodicity, a triangular lattice fits, whenever the stripe width d (with the stripe orientation given by $\vec{A}(j,k)/|\vec{A}(j,k)|$) and the interstripe distance b have periodicity $\xi(j,k)$, $j,k \in Z$,

$$b+d = \xi(j,k). \tag{15}$$

This introduces a linear relationship between stripe width d and interstripe distance b. In the b-d plane, lines joining $(\xi,0)$ and $(0,\xi)$ indicate regions where the triangular lattice fits the stripe pattern. For smaller values of ξ, these lines get increasingly dense and finally converge into the origin.

The assumption of $b+d$ periodicity is not mandatory. Rather, we could let the structure be periodic after m lattice spacings $\xi(j,k)$, and after l stripe spacings $(b+d)$. This relation reads

$$b+d = \frac{m}{l}\xi(j,k), \tag{16}$$

where m and l must be undivisible integers, in order to avoid redundances. The periodicity brings about a set of inequalities to be satisfied, expressing the condition that no sphere may lie outside a stripe,

$$i\xi(j,k) \leqslant j(b+d) \vee i\xi(j,k) \geqslant j(b+d)+b, \tag{17}$$

that is to be fulfilled for all i,j. Solving this leads to the relation

$$(m-1)b \leqslant d. \tag{18}$$

If we assume equality and use Eq. (16), we can solve for the minimal stripe width $d_{\min}$ and simultaneous maximal interstripe distance $b_{\max}$. These are

$$b_{\max}=\frac{1}{l}\xi(j,k), \tag{19}$$

$$d_{\min}=\frac{(m-1)}{l}\xi(j,k), \tag{20}$$

and fulfill the relation

$$(m-1)b_{\max}=d_{\min}. \tag{21}$$

Hence the triangular regimes are lines from $(0,\xi)$ to $(b_{\max},d_{\min})$. The above case [lines from $(0,\xi)$ to $(\xi,0)$] is recovered for $m=l=1$. For each combination of m and l we thus get a one-dimensional regime, where the triangular lattice fits. Variation of j and k, at fixed m and l, then gives additional lines, shifted on the d axis with their length being reduced. This is illustrated in Fig. 5(a), where j and k are varied with $m=1$ and $l=1$ fixed (solid lines) as well as $m=4$ and $l=1$ fixed (dashed lines). The shift of the lines is according to Eq. (21), their upper end points lying on a line defined by Eq. (19), whose slope changes with m. In Fig. 5(b), the lattice line distances $\xi(j,k)$ are fixed via $j=0,k=1$ (solid lines), $j=0,k=2$ (dotted lines); and $j=1,k=2$ (dash-dotted lines), while m and l are varied. Figure 5(b) illustrates that (j,k) for a given combination of (m,l) determine the height and position of one line, with other combinations of (m,l) producing replicas that are shifted on the d axis. Figure 5(c) covers the full range (relevant for the scale of the plot) of values j,k,m,l. Note how the lines get denser for $b\to 0$, and ultimately approach stripe-free bulk packing. Although we cannot prove that the triangular lattice does *not* fit any other parts in the phase diagram, we find that quite likely.

The geometrical features of the regimes are visually quite striking and may be unexpected from the outset. It is, however, known that competition of length scales may induce fractal structures [60]. One simple tool to analyze these is box counting [61]. In a two-dimensional situation, one covers the structure under consideration with a rectangular mesh with mesh width W, and counts the number of boxes, B, that touch (or are completely inside) the structure. This is performed successive times on smaller length scales W. For a fractal, a scaling law $B\propto W^{-\gamma}$ holds, where the dimension γ is not an integer. We have carried out such an analysis and could confirm quite well power law scaling with a noninteger exponent. A precise determination of γ, however, turned out to be subtle. We have restricted ourselves to a physically reasonable lower cutoff $W>10^{-3}\sigma$. For $m=l=1$, we obtain a $\gamma=1.5$. Superimposing ''fence'' patterns by varying m,l over a broad range of values changes the dimension to $\gamma=1.6$. Such an increase seems reasonable, as apparently, the structure gets denser. We leave a more thorough investigation to possible future research.

2. More general cases

We will approach the general case by considering interacting stripes that are themselves densely packed. Results are known for $b/\sigma>1$, periodic arrangement of the stripes will, however, give rise to special lattices. For $b/\sigma=1$, the spheres from different stripes can touch and the stable phase is determined by the equilibrium structure on the stripes, together with the degeneracy breaking condition $v_0/\epsilon\to 0^-$. We thus get *quadratic* ordering in the interstripe region. A pure quadratic lattice is stable only in one point: $b/\sigma=d$ and $d=0$. For lower b and $d=0$ it gets distorted to a lattice of alternating rhombi, as illustrated in Fig. 6(a). For $d<\sqrt{3}\sigma/2$ the situation is sketched in Figs. 6(b)–6(d) for decreasing values of b. Figure 6 (b) shows $1\mathcal{S}$ structures on decoupled stripes forming kite-structures in a periodic stripe arrangement. The kite structure of Fig. 6(b), however, is degenerated with respect to an arbitrary relative shift of two single stripe patterns. Upon approach and coupling of the stripes a honeycomb (HC) in Fig. 6(c), and eventually a

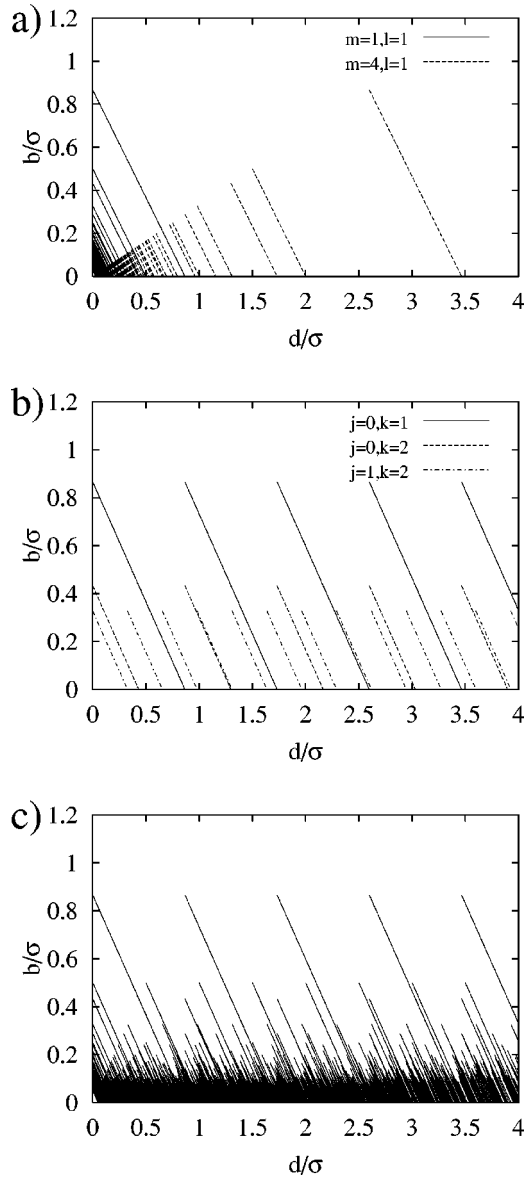

FIG. 5. Regions of stability of the triangular lattice (lines). (a) m,l kept constant (as indicated), and j,k varied. (b) i,j kept constant (as indicated), and m,l varied. (c) Full range of j,k,m,l (relevant for the scale of the plot).

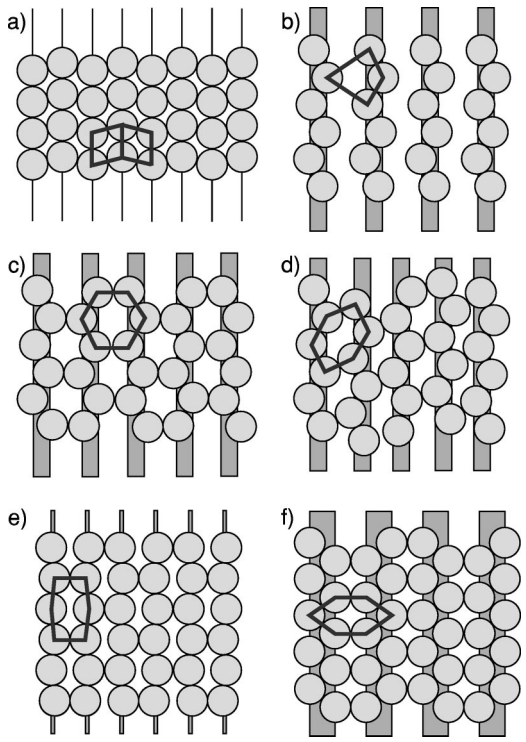

FIG. 6. Crystal structures for $d/\sigma < \sqrt{3}/2$. (a) Alternating rhombic for $d=0$ and $\sqrt{3}/2 < b/\sigma < 1$; in (b)–(d) the situation is shown for $0 < d/\sigma < \sqrt{3}/2$ for decreasing values of the interstripe width b/σ; (b) $1\mathcal{S}$ structures on decoupled stripes giving rise to kite structures in a periodic stripe arrangement; (c) honeycomb (1HC); (d) sheared honeycomb (sheared 1HC); (e) and (f): squeezed 1HC for $b/\sigma=1$, with $d/\sigma<0.5$ and $d/\sigma>0.5$, respectively. Solid lines indicate unit cells.

sheared honeycomb, shown in Fig. 6(d), emerge. For still smaller b, we expect another alternating rhombic phase, as shown in Fig. 6(a), but with finite $d>0$, to be stable.

For infinitely thin stripes, the situation for decreasing interstripe distances b is sketched in Fig. 7. A sequence of triangular lattices and centered rectangular lattices arises. Similar structures were observed in recent experiments [29,33].

For large $d>\sqrt{3}\sigma/2$, a squeezed honeycomb structure [Fig. 8(a)] that can also be sheared [Fig. 8(b)] appears. More complex crystal unit cells involving two supertriangular honeycomb structures, both sheared [Fig. 8(c)] and unsheared [Fig. 8(d)] occur for even larger d.

The resulting phase diagram of possible decoration lattices as a function of b/σ and d/σ is depicted in Fig. 9. While for $b/\sigma>1$ supertriangles are stable (compare Fig. 4), a cascade of sheared honeycomb phases consisting of supertriangles occurs for $b/\sigma<1$ and increasing d. Along coexistence lines (dashed lines in Fig. 9), these sheared supertriangle honeycomb phases degenerate into different special cases: square lattice $(d/\sigma=0, b/\sigma=0)$, unsheared honeycomb, squeezed honeycomb [see Figs. 6(e) and 6(f)], and alternating rhombic.

We combine the main results of this investigation with the regions of stability of the undistorted triangular lattice (Sec. IV B 1) and display the whole phase diagram of possible

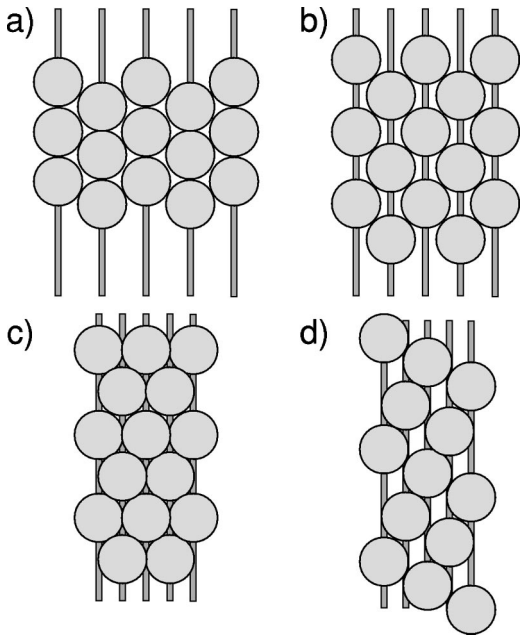

FIG. 7. Crystal structures for infinitely thin stripes $d/\sigma=0$ and decreasing values of b/σ: (a) hexagonal lattice $(b/\sigma=\sqrt{3}/2)$; (b) centered rectangular $(0.5<b/\sigma<\sqrt{3}/2)$; (c) hexagonal lattice $(b/\sigma=0.5)$; (d) centered rectangular $(b/\sigma<0.5)$.

decoration lattices as a function of b/σ and d/σ in Fig. 10. The states between the lines of stability of the triangular lattice are unexplored in our study. We leave those to future work.

Figures 9 and 10 prove that even though our model is relatively simple, competition of different length scales leads to quite different stable decoration lattice structures. On the basis of Figs. 9 and 10 one can tailor the attractive stripe pattern in order to produce a given decoration lattice. This is of direct importance for further crystal growth on top of the

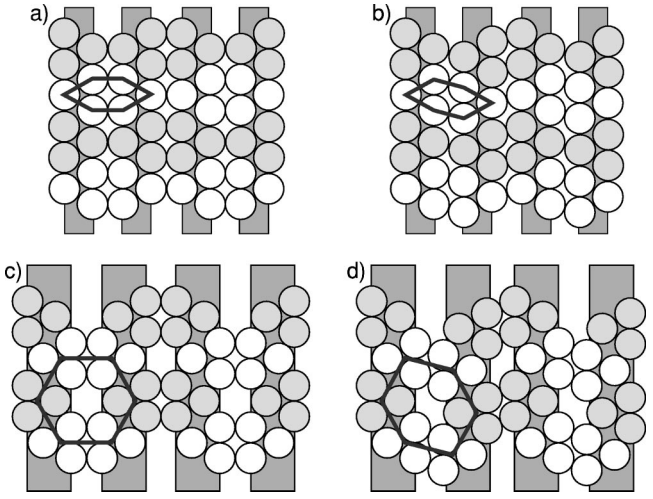

FIG. 8. Crystal structures for $\sqrt{3}/2 \leqslant d/\sigma < \sqrt{3}$ and $b/\sigma \leqslant 1$: (a) 2Δ-square hybrid; (b) sheared 2Δ-square hybrid; (c) two-honeycomb structure (2HC); (d) sheared two-honeycomb (sheared 2HC). Spheres building equilateral triangles are shaded to guide the eye. Solid lines indicate unit cells.

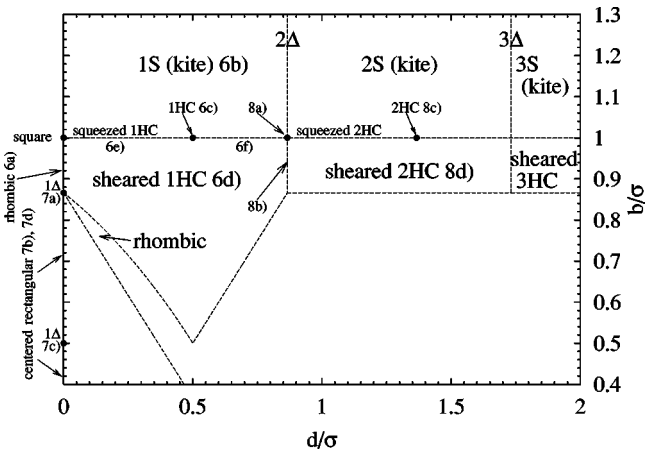

FIG. 9. Phase diagram of attractive hard spheres in a periodic arrangement of sticky stripes with stripe width *d* and interstripe separation *b*. Dashed lines indicate two-phase coexistence. Various crystals are stable, as displayed in Figs. 6–8.

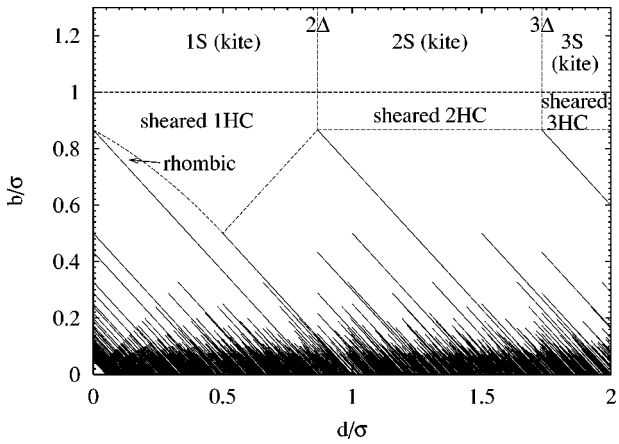

FIG. 10. Phase diagram of attractive hard spheres in a periodic arrangement of sticky stripes with stripe width *d* and interstripe separation *b*. Solid lines indicate triangular regimes, dashed lines indicate two-phase coexistence.

decoration lattice used as a template. One can expect [16] that quite exotic bulk crystalline structures can be aggregated on top of such a template [32]. This is of relevance for the construction of optical band-gap materials such as photonic crystals [62].

V. CONCLUSION

In conclusion, we have systematically investigated and predicted decoration lattices composed of colloidal particles adsorbed on an attractive stripe-patterned substrate. Our results show, that due to a competition of various length scales, a wealth of different decoration lattices can be stable. This knowledge can be exploited to generate exotic lattice structures by a tailored surface pattern that could be of relevance for fabricating photonic crystals grown on such templates. Our work can be extended into several directions: First, other periodic patterns such as alternating triangular or chessboard patterns can be studied, where even more complicated decoration lattices are expected. Second, the effect of finite temperature and longer ranged and more realistic particle-particle and particle-wall interaction should be investigated. Still we think that the main possibility of decoration lattices will be very similar to the results obtained for the more simplistic interactions. Also, the nonequilibrium problem of particle deposition can produce even much richer nonequilibrium fractal and random closed-packing structures [63–66] that have not been considered in the present equilibrium study. Finally, proving rigorously the different structures to be close packed should be an interesting problem in mathematical geometry.

ACKNOWLEDGMENTS

We thank A. Esztermann, C. N. Likos, and C. von Ferber for helpful remarks. This work was supported by the DFG within the wetting priority program under Contract No. LO 418/5-3.

[1] For a recent review see: Y. Xia, D. Qin, and Y. Yin, Curr. Opin. Colloid Interface Sci. **6**, 54 (2001).
[2] S. Friebel, J. Aizenberg, S. Abad, and P. Wiltzius, Appl. Phys. Lett. **77**, 2406 (2000).
[3] P. Lenz and R. Lipowsky, Phys. Rev. Lett. **80**, 1920 (1998).
[4] P. Lenz and R. Lipowsky, Eur. J. E **1**, 249 (2000).
[5] S. Herminghaus, A. Fery, S. Schlagowski, K. Jacobs, R. Seemann, H. Gau, W. Mönch, and T. Pompe, J. Phys.: Condens. Matter **12**, A57 (2000).
[6] C. Bauer and S. Dietrich, Phys. Rev. E **60**, 6919 (1999).
[7] L. J. Frink and A. G. Salingers, J. Chem. Phys. **110**, 5969 (1999).
[8] H. Bock and M. Schoen, Phys. Rev. E **59**, 4122 (1999).
[9] H. Bock and M. Schoen, J. Phys. Condens. Matter **12**, 1569 (2000).
[10] R. Lipowsky, Curr. Opin. Colloid Interface Sci. **6**, 40 (2001).
[11] J. Aizenberg, P. V. Braun, and P. Wiltzius, Phys. Rev. Lett. **84**, 2997 (2000).
[12] T. R. Weikl and R. Lipowsky, Langmuir **16**, 9338 (2000).
[13] H. Clausen-Schaumann and H. E. Gaub, Langmuir **15**, 8246 (1999).
[14] A. Sanjoh and T. Tsukihara, J. Cryst. Growth **196**, 691 (1999).
[15] J. Aizenberg, A. J. Black, and G. M. Whitesides, Nature (London) **398**, 495 (1998).
[16] M. Heni and H. Löwen, Phys. Rev. Lett. **85**, 3668 (2000).
[17] M. Heni and H. Löwen, J. Phys.: Condens. Matter **13**, 4675 (2001).
[18] M. Böltau, S. Walheim, J. Mlynek, G. Krausch, and U. Steiner, Nature (London) **391**, 877 (1998).
[19] B. H. Weigl and P. Yager, Science **283**, 346 (1999).
[20] H. Gau, S. Herminghaus, P. Lenz, and R. Lipowsky, Science **283**, 46 (1999).

[21] F. Burmeister, W. Badowsky, T. Braun, S. Wieprich, J. Boneberg, and P. Leiderer, Appl. Surf. Sci. **145**, 461 (1999).
[22] F. Burmeister, C. Schäfle, B. Keilhofer, C. Bechinger, J. Boneberg, and P. Leiderer, Chem. Eng. Technol. **21**, 761 (1998).
[23] C. Mio and D. W. M. Marr, Langmuir **15**, 8565 (1999).
[24] K. M. Chen, X. Jiang, L. C. Kimerling, and P. T. Hammond, Langmuir **16**, 7825 (2000).
[25] C. A. Murray, Abstr. Pap.-Am. Chem. Soc. **220**, 74 (2000).
[26] K. Mangold, R. Bubeck, P. Leiderer, and C. Bechinger, Prog. Colloid Polym. Sci. **118**, 77 (2001).
[27] Z. Adamczyk, B. Siwek, and E. Musial, Langmuir **17**, 4529 (2001).
[28] Q. Guo, C. Arnoux, and R. E. Palmer, Langmuir **17**, 7150 (2001).
[29] Y.-H. Ye, S. Badilescu, V.-V. Truong, P. Rochon, and A. Natansohn, Appl. Phys. Lett. **79**, 872 (2001).
[30] A. Chowdhury, B. J. Ackerson, and N. A. Clark, Phys. Rev. Lett. **55**, 833 (1985).
[31] A. K. Arora and R. Rajagopalan, Curr. Opin. Colloid Interface Sci. **2**, 391 (1997).
[32] A. van Blaaderen, R. Ruel, and P. Wiltzius, Nature (London) **385**, 321 (1997).
[33] K. hui Lin, J. C. Crocker, V. Passad, A. Schofield, D. A. Weitz, T. C. Lubensky, and A. G. Yodh, Phys. Rev. Lett. **85**, 1770 (2000).
[34] F. Burmeister, C. Schäfle, T. Matthes, M. Bohmisch, J. Boneberg, and P. Leiderer, Langmuir **13**, 2983 (1997).
[35] C. Rotsch and M. Radmacher, Langmuir **13**, 2825 (1997).
[36] S. J. Miklavic, D. Y. C. Chan, L. R. White, and T. W. Healy, J. Phys. Chem. **98**, 9022 (1994).
[37] J. Hu and R. M. Westervelt, Phys. Rev. B **55**, 771 (1997).
[38] P. Meakin and R. Jullien, Physica A **175**, 211 (1991).
[39] P. N. Pusey, in *Liquids, Freezing and the Glass Transition*, edited by J. P. Hansen, D. Levesque, and J. Zinn-Justin, Les Houches Lectures, Vol. 51 (North Holland, Amsterdam, 1991), p. 763.
[40] P. Bolhuis, M. Hagen, and D. Frenkel, Phys. Rev. E **50**, 4880 (1994).
[41] C. N. Likos, Z. T. Németh, and H. Löwen, J. Phys.: Condens. Matter **6**, 10 965 (1994).
[42] A. R. Denton and H. Löwen, J. Phys.: Condens. Matter **9**, L1 (1997).
[43] P. Bolhuis and D. Frenkel, J. Phys.: Condens. Matter **9**, 381 (1997).
[44] A. Patrykiejew, S. Sokolowski, and K. Binder, J. Chem. Phys. **115**, 983 (2001).
[45] A. R. Denton and H. Löwen, Phys. Rev. Lett. **81**, 469 (1998).
[46] L. Levitov, Phys. Rev. Lett. **66**, 224 (1991).
[47] S. Neser, C. Bechinger, P. Leiderer, and T. Palberg, Phys. Rev. Lett. **79**, 2348 (1997).
[48] M. Schmidt and H. Löwen, Phys. Rev. Lett. **76**, 4552 (1996).
[49] M. Schmidt and H. Löwen, Phys. Rev. E **55**, 7228 (1997).
[50] M. Leppmeier, *Kugelpackungen: Von Kepler bis Heute* (Vieweg, Wiesbaden, 1997).
[51] H. Löwen, in *Spatial Statistics and Statistical Physics*, edited by K. Mecke and D. Stoyan, Lecture Notes in Physics Vol. 554 (Springer, Berlin, 2000), p. 295.
[52] R. Peikert, El. Math. **49**, 17 (1994).
[53] H. Melissen, El. Math. **49**, 27 (1994).
[54] R. K. Bowle and R. J. Speedy, Physica A **262**, 76 (1999).
[55] H. Melissen, Am. Math. Monthly **100**, 916 (1993).
[56] H. Melissen, Acta Math. Hung. **65**, 389 (1994).
[57] H. Melissen, Geometria Dedicata **50**, 15 (1994).
[58] B. D. Lubachevsky and R. L. Graham, Discrete. Comput. Geom. **18**, 179 (1997).
[59] Z. T. Németh and H. Löwen, J. Phys.: Condens. Matter **10**, 6189 (1998).
[60] P. M. Chaikin and T. C. Lubensky, *Principles of Condensed Matter Physics* (Cambridge University Press, Cambridge, U.K., 2000).
[61] K. J. Falconer, *Fractal Geometry, Mathematical Foundations and Applications* (Wiley, New York, 1990).
[62] C. E. Reese, C. D. Guerrero, J. M. Weissman, K. Lee, and S. A. Asher, J. Colloid Interface Sci. **232**, 76 (2000).
[63] P. Meakin and R. Jullien, Europhys. Lett. **15**, 667 (1991).
[64] P. Meakin and R. Jullien, Europhys. Lett. **15**, 851 (1991).
[65] B. D. Lubachevsky, F. H. Stillinger, and E. N. Pinton, J. Stat. Phys. **64**, 501 (1991).
[66] J. E. Socolar, Europhys. Lett. **18**, 39 (1992).